Zeitschrift: Helvetica Physica Acta
Band: 43 (1970)
Heft: 2

Artikel: A study on bubble formation in the bubble chamber
Autor: Poesposoetjipto, F.H. / Hugentobler, E.
DOI: https://doi.org/10.5169/seals-114165

A Study on Bubble Formation in the Bubble Chamber

by **F. H. Poesposoetjipto** and **E. Hugentobler**
University of Fribourg, Switzerland

(14. XI. 69)

Abstract. Experimental study on the bubble formation has been performed using a temperature and pressure stabilized bubble chamber. The bubble formation by high energy ionizing particles has been studied for $CBrF_3$ at 25.9 °C, 28.8 °C and 32.4 °C. Furthermore, the bubble formation by α-decay-recoils has been investigated for $CBrF_3$, CCl_2F_2 and C_3F_8 in the temperature range 20 to 60 °C. It has been found qualitatively that from both experiments the energy needed for the bubble formation should be deposited in a volume of subcritical dimension. Light-induced bubble formation has been observed and the results are described.

1. Introduction

Since the invention of the bubble chamber, several studies have been conducted on the bubble formation mechanism, either theoretically or experimentally [1–11]. The general understanding on the formation of bubbles in the bubble chamber is based on the assumption that a minute amount of energy in the form of heat is brought to a small region in the metastable liquid and thereby provokes the initial ruptures in the liquid. There are still many problems to be clarified concerning the mechanism by which the bubbles are created in the liquids of different physical and chemical properties and composition. It is the purpose of this study to present the experimental results on the bubble formation in CCl_2F_2, $CBrF_3$ and C_3F_8.

Riepe et al. [2] have performed an experiment in C_3H_8 and CCl_2F_2 on the bubble formation in the bubble chamber using the α-decay-recoils. Their results seem to indicate that the bubble chamber shows a 100% efficiency for the α-decay-recoils if the degree of superheat in the liquid is large enough. The bubble formation induced by high-energy particles on the other hand has been assumed to be created by the δ-electrons. Kunkel [3] has studied systematically the formation of bubbles in a propane bubble chamber using high-energy electrons. He found that for a sufficiently large degree of superheat the efficiency of the δ-electrons for the bubble formation tends to approach one.

In this study, experiments on the bubble formation have been performed with the aid of the α-decay-recoils and of high-energy protons. The recoiling atom used in this study was Pb^{206} which is obtained from the α-disintegrating Po^{210} isotope. The proton energy was 21.6 GeV.

With the advent of the laser, experiments were conducted on the bubble formation induced by intense light. Hugentobler et al. [12] have shown that in the beam of

the laser pulse, bubbles were created. Stamberg et al. [13] found the same effect and they explained that lint and dust particles, which absorb light at 6943 Å are the source of nucleation.

2. Experimental Methods

2.1 *Bubble chamber*

The bubble chamber used for the investigation is described by Hahn et al. [14] and Riepe et al. [2]. The final pressure of the expansion can be kept at a desired pressure by using a stabilization tank, which is filled with compressed air of the desired final pressure p_s. The pressure drop, i.e. the pressure difference between the saturation pressure of the liquid p_∞ and the final pressure p_s, $\Delta p = p_\infty - p_s$, was determined by means of a differential manometer. The one end of the differential manometer was connected to a reference liquid chamber, which was filled with the same liquid and held at the same temperature as the liquid in the bubble chamber. The other end of the differential manometer was connected to the stabilization tank. The dynamics of the pressure drop $\Delta p' = p_0 - p_s$ was followed by a quartz crystal pressure transducer (SLM type PZ14). The induced electrostatic charge of the pressure transducer was amplified and fed to an oscilloscope. p_0 is the overpressure and was chosen to be approximately 5 atmospheres above the saturation pressure p_∞ of the liquid.

The temperature of the bubble chamber liquid and the reference liquid was regulated and held constant with temperature-stabilized water, which flowed through the pores in the chamber body, the stabilization tank and the reference chamber body. The temperature and temperature variations of the liquid were measured with Fe-Constantan thermocouples. The temperature variation in the liquid of the bubble chamber during the experiment is of the order of $\pm$ 0.1 °C.

2.2 *Exposure of the bubble chamber to high-energy particles*

The bubble chamber was exposed to a proton beam of 21.6 GeV at the proton-synchrotron at CERN, Geneva. In traversing the chamber, these particles leave traces along their path in the form of microscopic bubbles. Those microscopic bubbles, which reach the critical size, grow further to visible size without outside energy supply.

During their growth the adjacent bubbles can coalesce into one single bubble. The recorded bubbles on the film give thus an apparant bubble density $N'(T, \Delta p)$, which is always smaller than the physically important bubble density $N(T, \Delta p)$ of the created critical bubble.

The bubble density $N(T, \Delta p)$ was determined by the 'distribution of the gap length'-method, as it is described by Hugentobler et al. [4].

2.3 *Recoiling atoms as an energy supply for the bubble formation*

Using a definite monoenergetic recoiling atomic nucleus as an energy supplier, it would be expected that at a certain value of the pressure drop Δp bubbles start to be created and an increase of the pressure drop has the effect that all recoils create bubbles. It was found that the recoil of Pb^{206} in the α-decay of Po^{210} [1]), which is

[1]) The Po^{210} was supplied by the Radiochemical Centre in Amersham.

Pb^{206} with a recoil energy of 103 keV would be suitable for the intended investigation on the bubble formation.

Due to the short range of the recoiling atom it is necessary to introduce the α-active substance in a solution form into the chamber liquid. Since the liquids used in this investigation are organic compounds, it was necessary to find an organic polonium compound soluble in a solvent, which can be mixed with the chamber liquids. It turned out that the polonium carbamate complex is soluble in CCl_4, which in turn can be mixed with the chamber liquids in reasonable quantity. The content of the solvent CCl_4 with the polonium carbamate complex in the chamber liquid was kept at less than 1%. The polonium carbamate was prepared according to the description by Guillot [15].

Pictures of the bubbles were taken during the time in which the final pressure p_s was constant (which is also called the 'pressure plateau'). The bubbles were photographed at a time delay t, as indicated in Figure 1.

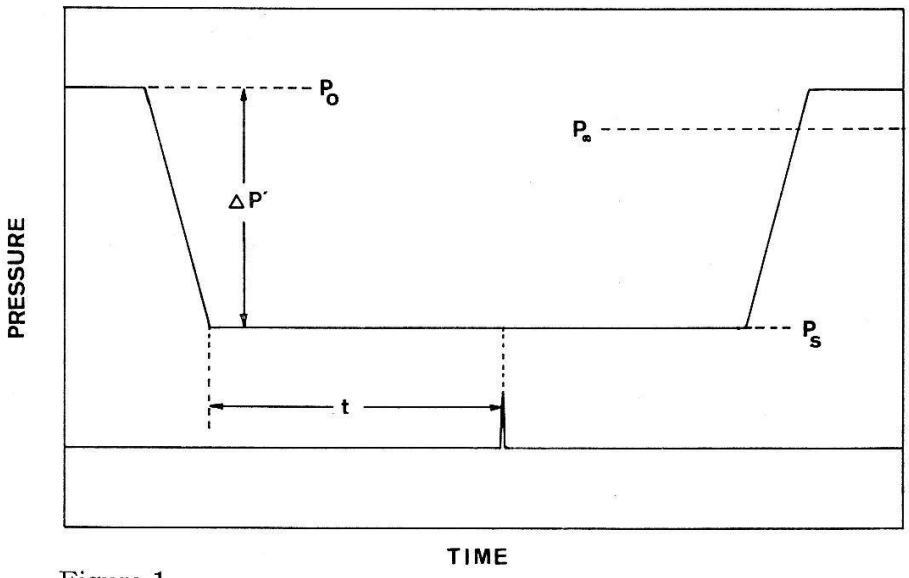

Figure 1
Schematic representation of the dynamics of the pressure drop. p_0 is the overpressure. p_∞ is the saturation pressure of the liquids. p_s is the final pressure and t is the time delay.

Within the pressure plateau, the number of bubbles increases linearly with increasing time delay t [2]. For a certain given pressure drop value Δp the liquid was expanded several times and at each expansion pictures of the bubbles with varying time delay were taken. The number of bubbles $N_b(T, \Delta p)$ created per unit time was then determined by applying the least-square-method to the counted number of bubbles as a function of the time delay t. To avoid the bubbles which are created by the imperfections of the chamber wall, a mask was used in the determination on the number of bubbles.

2.4 *Exposure of the bubble chamber to high intensity light source*

A spark type light source was used to investigate light induced bubble formation. A capacitor having a capacitance of 7.71 μF is charged with a potential of 15 kV. This corresponds to an energy of 867 joules.

This stored electrical energy was discharged through a spark gap and the discharge was initiated with a 10 kV triggerpulse. The discharge medium was air of atmospheric pressure.

The emitted light has an extended broad spectrum mostly from atomic nitrogen [16]. According to Glaser [17] it can be assumed that $\sim 2\%$ of the electrical energy stored in the capacitor during the discharge is converted into light energy. Consequently, the light energy obtained with the above-mentioned operating conditions is approximately 20 joules. Furthermore, the pulse light was collimated with a condenser with a solid angle of 3%. The discharge time of the spark light source was of the order of 30 μs. The resulting intensity of the light beam, which traversed the bubble chamber, was approximately 1.4×10^{23} eV/cm^{2}s. The light beam was a few mm wide.

3. Energy Required to Form a Critical Bubble

According to the thermal theory of bubble formation in a superheated liquid, the initial ruptures in the liquid are caused by the rapid heating of a small region, whose dimension is smaller than the critical size. In the bubble chamber the liquid is expanded to a stabilization pressure p_s. The degree of superheat (pressure drop) is then given by

$$\Delta p = p_v - p_s \tag{1}$$

where p_v denotes the pressure inside the bubble. According to Frenkel [18] the pressure inside a bubble of radius R in a liquid can be taken as equal to the saturation pressure (i.e. $p_v = p_\infty$).

Assuming that the bubble reaches the critical size within a time $\tau_c \leqslant \tau_w(R_c)$, where $\tau_w(R_c)$ is the time constant for the decay of a thermal 'spike' in the liquid and R_c is the critical bubble radius, the bubble can be considered as following an adiabatic process during its growth to the critical size. The minimal energy W_m required to form a bubble is then given by the sum of the static energetic terms comprising the surface work, the volume work and the evaporation heat [1–11].

$$W_m = 4\pi R_c^2 \left(\sigma - T \frac{\partial \sigma}{\partial T}\right) + \frac{4}{3} \pi R_c^3 (p_s + \varrho_v h) \tag{2}$$

where R_c, σ, T, p_s, ϱ_v and h denote the critical bubble radius, the surface tension, the absolute temperature, the stabilization pressure, the vapor density and the heat of evaporation per gram, respectively.

Figures 2 and 3 show the dependence of the minimal energy W_m required to form a bubble on the pressure drop and the critical radius for liquids used at 30.0 °C, respectively.

It is plausible to assume that the minimal energy W_m required to form a bubble should be deposited within a subcritical volume in the liquid. This subcritical volume is defined as a volume in which the number of the liquid molecules is equal to the number of the vapor molecules in the equilibrium critical volume. The radius of the subcritical volume is given by the following relation

$$R_0 = \left(\frac{\varrho_v}{\varrho_l}\right)^{1/3} R_c \tag{3}$$

where ϱ_l denotes the liquid density.

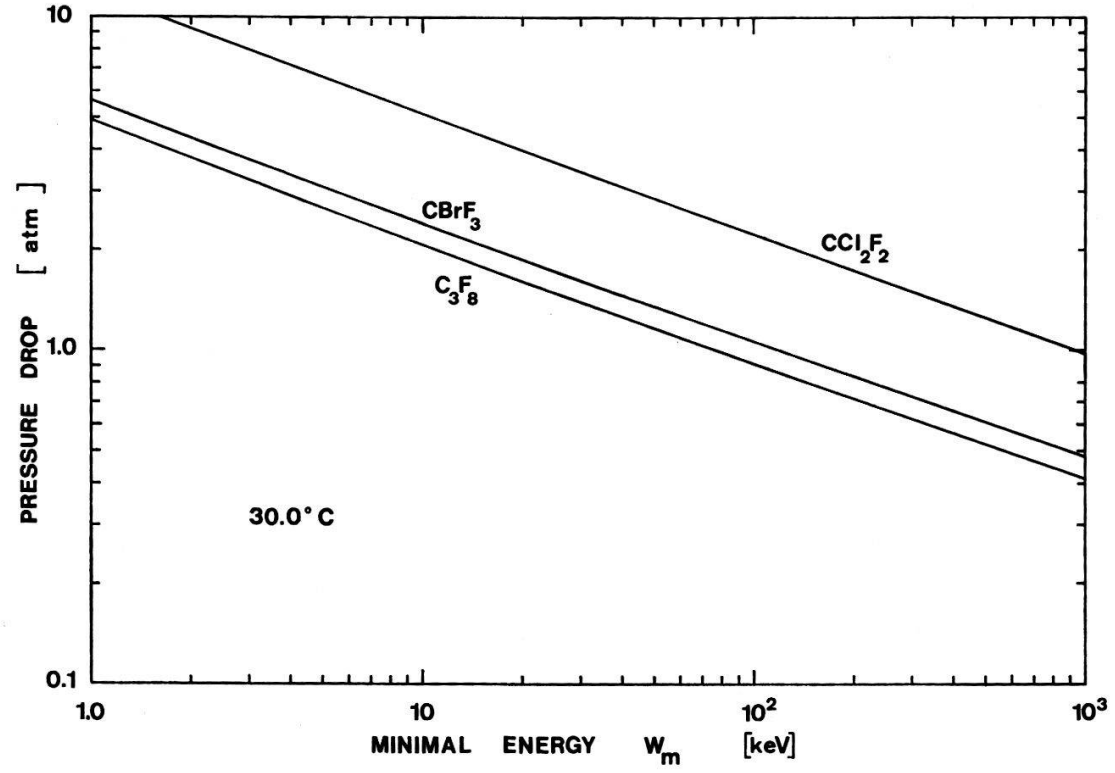

Figure 2
The dependence of the pressure drop on the minimal energy W_m required to form a bubble for liquids CCl_2F_2, $CBrF_3$ and C_3F_8 at 30.0 °C.

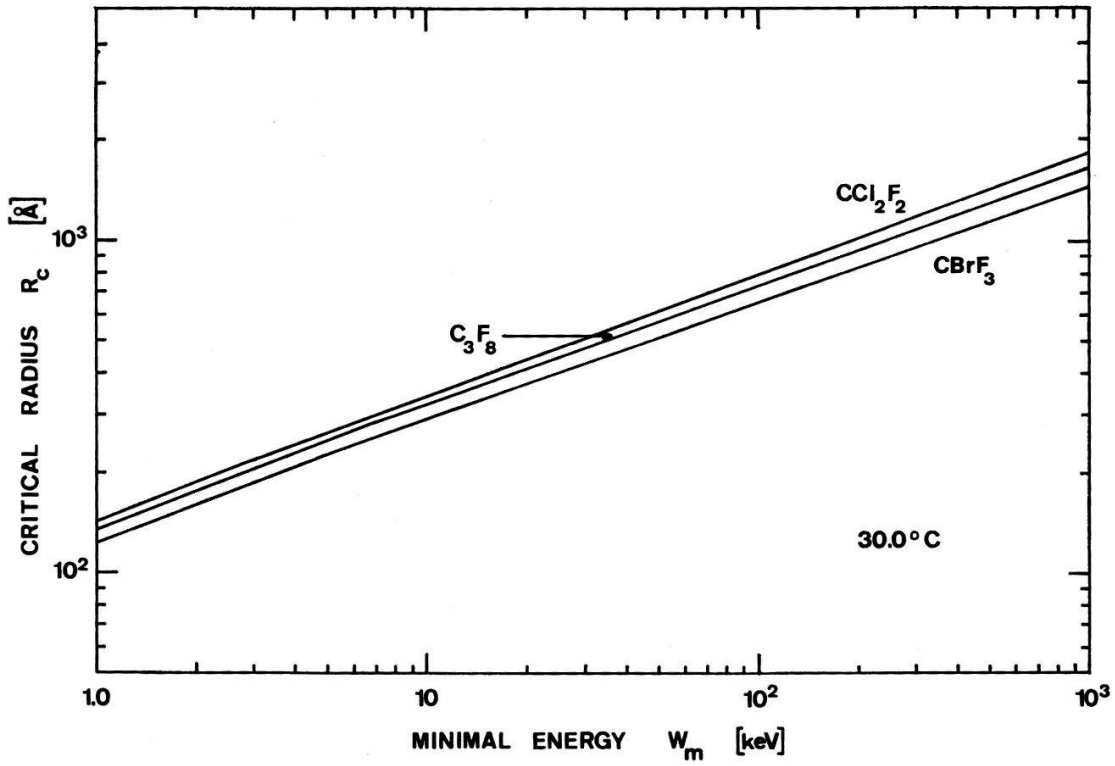

Figure 3
The dependence of the critical radius on the minimal energy W_m required to form a bubble for liquids CCl_2F_2, $CBrF_3$ and C_3F_8 at 30.0 °C.

The thermodynamic properties of the liquids used in this investigation are given by the data sheet [19–21]. The values of the surface tension were determined in this laboratory. The Katayama relation [22] was used to fit the experimental data of the surface tension. This relation is given by

$$\sigma = k\,(T_c - T)\left(\frac{\varrho_l - \varrho_v}{M}\right)^{2/3} \tag{4}$$

where k, T_c, T, M, ϱ_l and ϱ_v denote a constant, the critical temperature, the absolute temperature, the molecular weight, the liquid density and the vapor density, respectively. The value of the constant k is 2.12, 2.2 and 2.28 for CCl_2F_2, $CBrF_3$ and C_3F_8 respectively.

4. Discussion of the Experimental Results

4.1 *Bubble formation along the track of an ionizing highenergy particle*

A charged particle, which traverses the liquid, gives its energy to the atoms of the liquid through excitation and ionization. Starting from the assumption that only the δ-electrons are responsible for the thermal spike giving rise to primary bubbles in the bubble chamber liquid the problem is now to know the range of the δ-electrons and to find the number of these δ-electrons having kinetic energy at least equal to W_m.

The energy-range relation for low energy electrons (< 0.1 MeV) is not known as accurately as one would wish. Lea [23] has tabulated the range for electrons in the energy range of 0.1–480 keV in tissue, calculated according to the theory developed by Bethe [24]. The Bethe theory can be applied as long as the mean ionization potential is small compared to the electron energy. For the case of tissue this can be true since the mean ionization potential is ~ 45 eV. The mean ionization potential for $CBrF_3$ on the other hand is ~ 230 eV. Consequently, the electrons of energy ~ 100 eV are elastically scattered in $CBrF_3$. It is then expected that the range of these electrons should be larger than the values tabulated by Lea. But on the other hand these electrons are strongly multiple-scattered by the atoms that the path of these electrons is confined within a small volume. Assuming that both effects should compensate in $CBrF_3$ it is reasonable then to use the tabulated values of Lea for the range determination of the δ-electrons. This only should be taken as an order of magnitude statement. Figure 4 shows the dependence of the electron range, the critical bubble radius and the subcritical radius on the minimal energy W_m for $CBrF_3$ at 25.9 °C.

If $d\Phi/dE$ represents the differential ionization cross section for the creation of secondary electrons with energy from E to $E + dE$ and $w(E)$ represents the efficiency that a δ-electron of energy $E > W_m$ creates a critical bubble, the bubble density is then given by

$$N(T, \Delta p) = \int_{W_m}^{\infty} w(E)\,\frac{d\Phi}{dE}\,dE = \overline{w}(W_m)\,\Phi\,(E > W_m) \tag{5}$$

with

$$\Phi\,(E > W_m) = \int_{W_m}^{\infty} (d\Phi/dE)\,dE \tag{6}$$

where $\overline{w}(W_m)$ is the average efficiency for the bubble formation by the δ-electrons, which can be obtained from the experiments.

The differential ionization cross section for an atom has been analyzed theoretically by Møller [25]. The differential ionization cross section $d\Phi/dE$ for a liquid molecule is taken as the sum of the corresponding atomic cross sections. If the binding energy for an electron in an atom of the liquid is much less than W_m, such an electron can be considered as free. The differential ionization cross section for free electrons is given by

$$d\Phi/dE = \frac{2\pi e^4}{m_e c^2 \beta^2} \frac{N}{E^2} \tag{7}$$

where m_e, c, β, e and N denote the electron rest mass, the velocity of light, the velocity of the primary particle, the elementary charge and the number of electrons in a unit volume of the corresponding liquid.

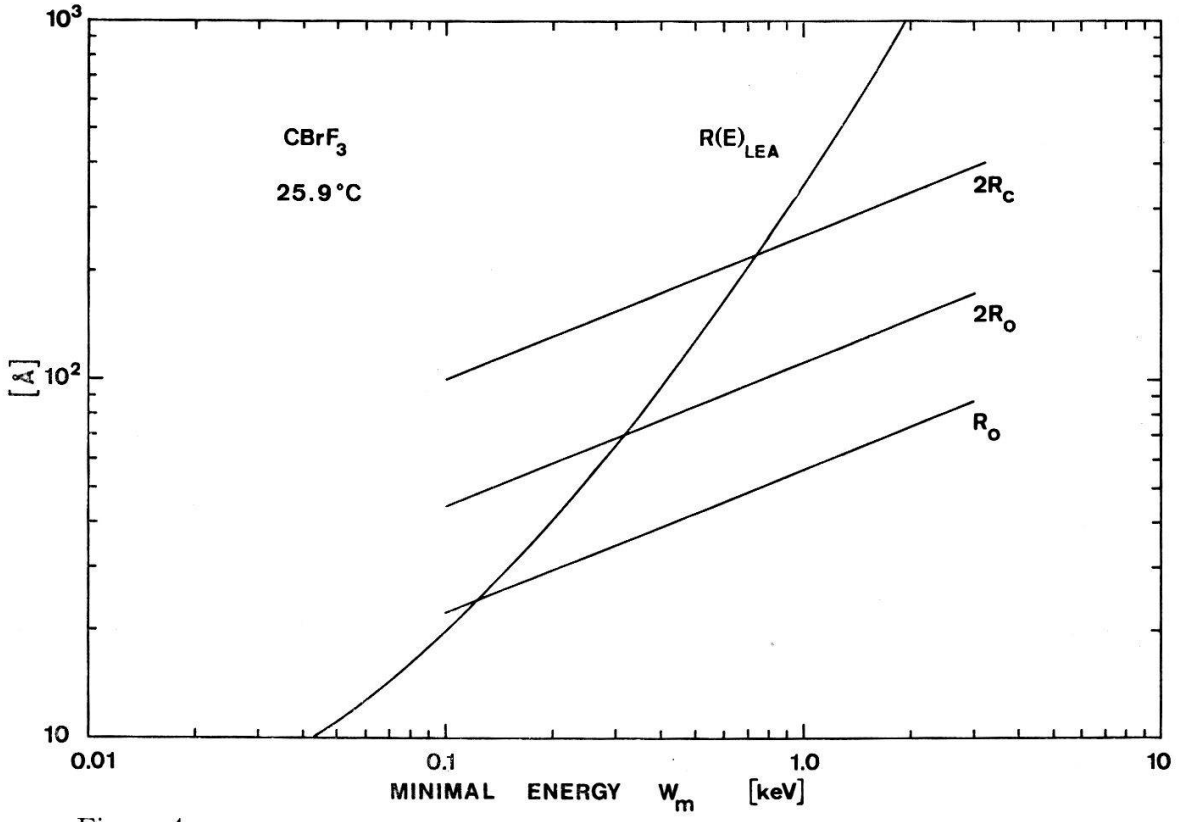

Figure 4
The dependence of the electron range obtained from the tabulated values of Lea, the critical bubble diameter, the subcritical bubble diameter and the subcritical radius on the minimal energy W_m for $CBrF_3$ at 25.9 °C.

In the case of $CBrF_3$ the binding energy of the electrons exceeds W_m and as such one can not consider the electrons as to be free. The differential ionization cross section for bound electrons $d\Phi/dE$ takes the following general form

$$\frac{d\Phi(E)}{dE} = \frac{A(E)}{\beta^2} [\ln(\gamma - 1) - \beta^2] + \frac{B(E)}{\beta^2} \tag{8}$$

where $A(E)$ and $B(E)$ are the γ-independent coefficients ($\gamma - 1 = E_k/m_0 c^2$, $m_0 =$ rest mass, $E_k =$ kinetic energy of the primary particle). The coefficients $A(E)$ and $B(E)$ have been calculated numerically by Hugentobler et al. [4]. The total differential ionization cross section $\Phi\,(E > W_m)$ is obtained by numerical integration according to (6). Figure 5 shows the total ionization cross section $\Phi\,(E > W_m)$ per centimeter for $CBrF_3$ along with experimental points at 25.9 °C. The experimental values at other temperatures are also drawn in the same figure by multiplying with ϱ_0/ϱ_l, because the number of δ-electrons is proportional to the density of the liquid. ϱ_0 is the density of the liquid at temperature T_0 (in this case $T_0 = 25.9\,°C$).

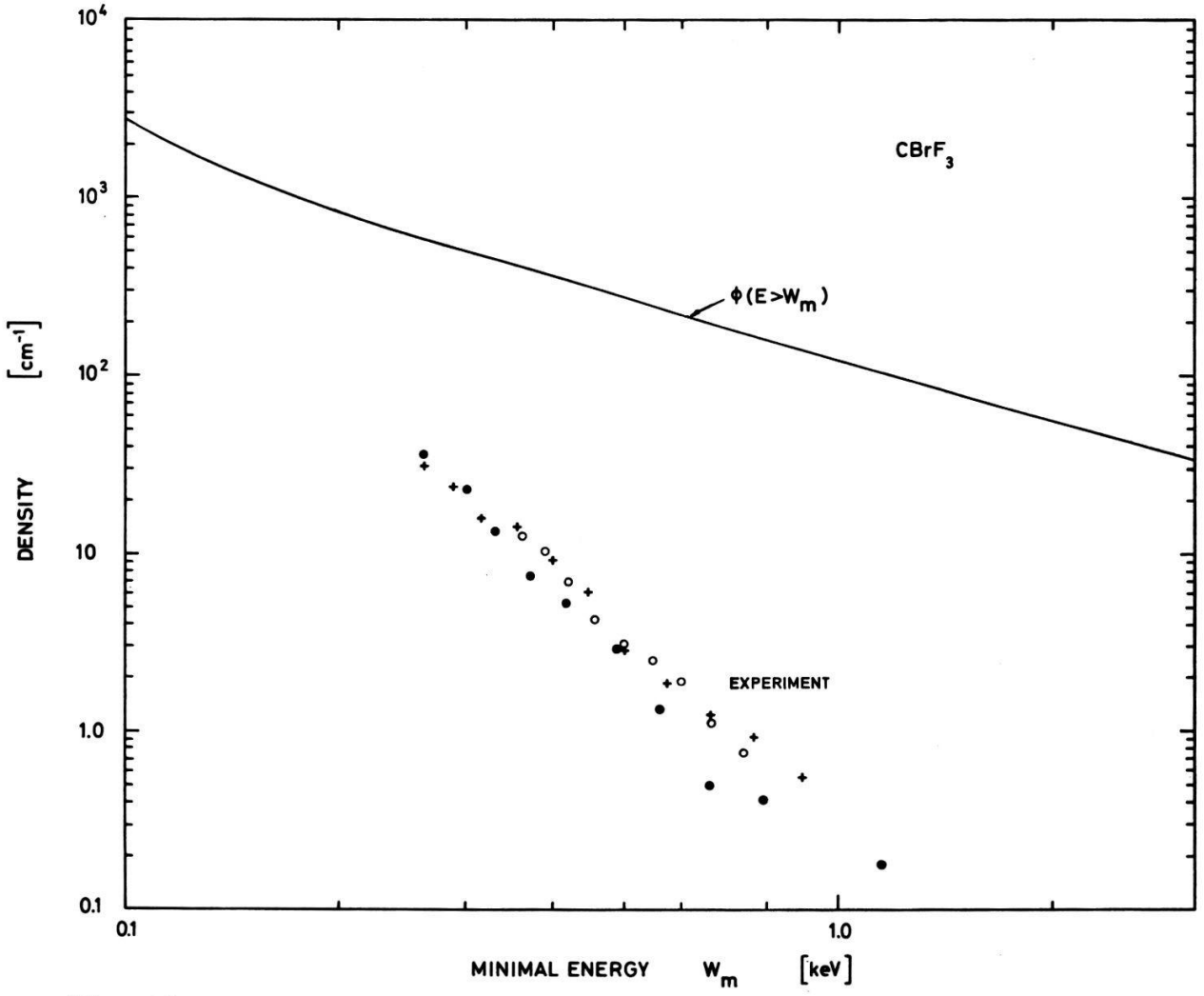

Figure 5
The total ionization cross section $\Phi\,(E > W_m)$ for the production of secondary electrons with kinematic energy $E > W_m$. ○ are the experimental bubble density at 25.9 °C. + are the experimental bubble density at 28.8 °C and ● are those at 32.4 °C.

The mean efficiency that a δ-electron of energy $E > W_m$ creates a critical bubble, is given by the relation (5). This efficiency $\overline{w}(E)$ is plotted as a function of the minimal energy W_m in Figure 6 for $CBrF_3$ at 25.9 °C. The ratio of the range of electrons as given by Lea [23] to the subcritical radius R_0 is also drawn in the same figure.

It is seen from Figure 6 that the efficiency $\overline{w}(E)$ extrapolated to lower energy approaches one in the same region, where the ratio between the range of the electrons and the subcritical radius R_0 becomes one. The above result seems to indicate that the energy supplied for the bubble formation should be contained within a volume of approximately R_0 diameter.

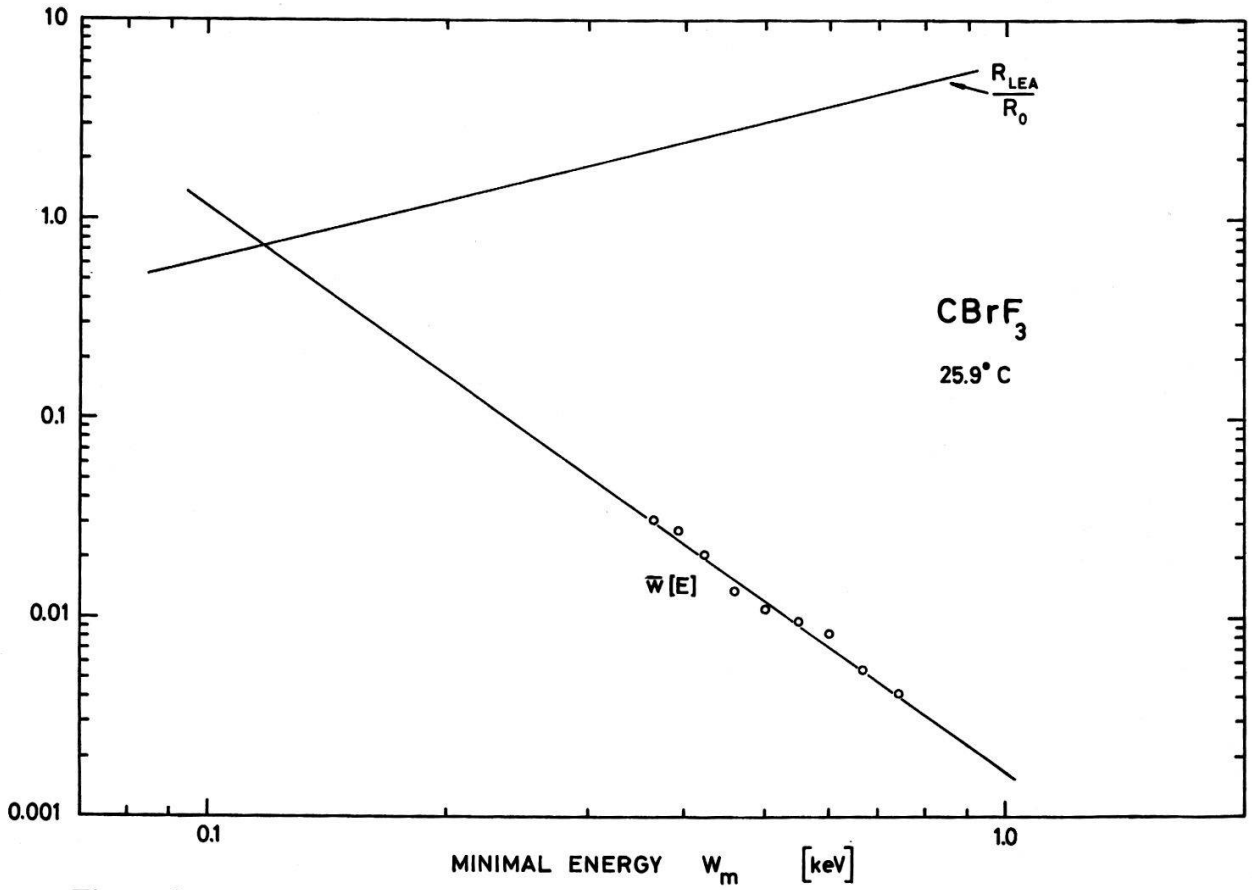

Figure 6
The mean efficiency $\overline{w}(E)$ of δ-electrons for the bubble formation in $CBrF_3$ at 25.9 °C as a function of the minimal energy required to form a critical bubble W_m. R_{Lea}/R_0 is the ratio between the range of electrons according to Lea to the subcritical radius.

Kunkel [3] found that for propane the efficiency reaches unity for an energy $E \sim 150$ eV. Applying the range-energy relation of Lea he found that the ratio between the range of electrons to the critical bubble diameter $2\,R_c$ reaches unity at approximately the same energy, i.e. $E \sim 150$ eV.

Due to the lack of a precise knowledge on the range-energy relation for slow electrons, it can only be concluded that the efficiency of the δ-electrons for bubble formation approaches one if the energy supplied by the δ-electrons is contained within a volume smaller or at the most equal to the critical volume.

4.2 *Bubble formation induced by alpha recoils*

When a recoiling atom moves in a liquid, it suffers a succession of scattering collision and loses energy to the atoms of the liquid. Bohr [26] has laid the theoretical foundation for the calculation of the stopping process in terms of elastic nuclear

collisions. His theory has since been extended and refined by Lindhard, Scharff and Schiøtt [27] and Biersack [28–29]. Lindhard et al. base their theoretical treatment on the Bohr-Thomas-Fermi statistical model, whereas Biersack has used the Thomas-Fermi-Firsov statistical model.

Several experiments have been performed to test the validity of the theories for low-energy ions [30–33]. It turned out that the theories of Lindhard et al. and Biersack agree very well with the experimental results. For high-energy ions ($E > 500$ keV) the experimental results lie between the theoretical predictions of Lindhard et al. and Biersack [34–35].

Assuming that the differential cross section for a molecule is obtained by an additive summation of the differential cross sections of the atomic constituents of the molecule, the total specific energy loss (dE/dR) for a molecule can be written as

$$dE/dR = \sum_i N_i \int T \, d\sigma = \sum_i N_i \, S_i \tag{9}$$

where N_i is the number of scattering centres per unit volume of the i-th atom of the molecule. $d\sigma$ is the differential cross section for an energy transfer T to atoms and atomic electrons. S is the stopping cross section per scattering centre.

Using the dimensionless measures for the range and energy as given by Lindhard et al. and Biersack, the stopping cross section, S_i, can be written as

$$S_i = 4\pi \, a \, e^2 \, Z_1 \, Z_i \frac{M_1}{M_1 + M_i} \left[\left(\frac{d\varepsilon}{d\varrho} \right)_{n_i} + \left(\frac{d\varepsilon}{d\varrho} \right)_{e_i} \right] \tag{10}$$

where a, e, Z_1, Z_i, M_1, M_i $(d\varepsilon/d\varrho)_{n_i}$ and $(d\varepsilon/d\varrho)_{e_i}$ denote the screening radius, the elementary charge, the charge number of the recoiling atom, the charge number of the atomic constituent of the molecule, the mass of the recoiling atom, the mass of the atomic constituent of the molecule, the dimensionless specific energy loss due to nuclear collision and the dimensionless specific energy loss due to the atomic electrons.

The values of $(d\varepsilon/d\varrho)_{n_i}$ for the nuclear collision are tabulated in the publication of Schiøtt [36] and in the paper of Biersack [28]. The specific energy loss due to electronic collision in our case can be neglected, since it contributes only a small correction.

The range can then be obtained by integration of the specific energy loss

$$R(E) = \int_0^E \frac{dE'}{(dE'/dR)} \, . \tag{11}$$

According to the theory of Bohr, the range of a recoiling atom in a liquid, whose velocity is small compared to the velocity of the electron in a hydrogen atom v_0 ($v_0 = e^2/\hbar = 2.2 \times 10^8$ cmsec^{-1}) and whose mass M_1 is very large compared to the mass of the molecules of the stopping medium, assuming the additive character of the differential cross section, can be written as

$$R_{\text{Bohr}} = \frac{e}{4\pi a_0^2} \frac{1}{Z_1 m_e} \left(\frac{v_R}{v_0} \right)^2 \frac{1}{N} \left(\sum_i \frac{c_i \, Z_i}{(M_1 + M_i)(Z_1^{2/3} + Z_1^{2/3})^{1/2}} \right)^{-1} \tag{12}$$

where c_i, e, v_0, v_R and a_0 denote the number of atoms of the same charge and mass in a molecule, the base of natural logarithm, the velocity of the electron in a hydrogen

atom, the velocity of the recoiling atom and the Bohr's atomic hydrogen radius, which is given by

$$a_0 = \frac{\hbar}{e^2 m_e} = 0.529 \text{ Å} .$$

The total range of the recoiling atom is then obtained by numerical integration of the total specific energy loss (dE/dR). The calculation was executed with the CDC 6400 computer at CERN.

Of interest here is to know the path length of the recoiling atom after losing an energy $\Delta E = E_m - E$, where E_m is the energy of the recoiling atom at the start. This path length is defined as

$$L(E) = \int_{E}^{E_m} \frac{dE'}{(dE'/dR)} . \tag{13}$$

In Figure 7 the path lengths $L(E)$ for the recoiling Pb^{206} atom are presented as calculated according to the theories of Bohr, Lindhard et al. and Biersack as a function of the minimal energy W_m. The critical bubble diameter, the subcritical bubble diameter and the subcritical radius are also drawn in the figure.

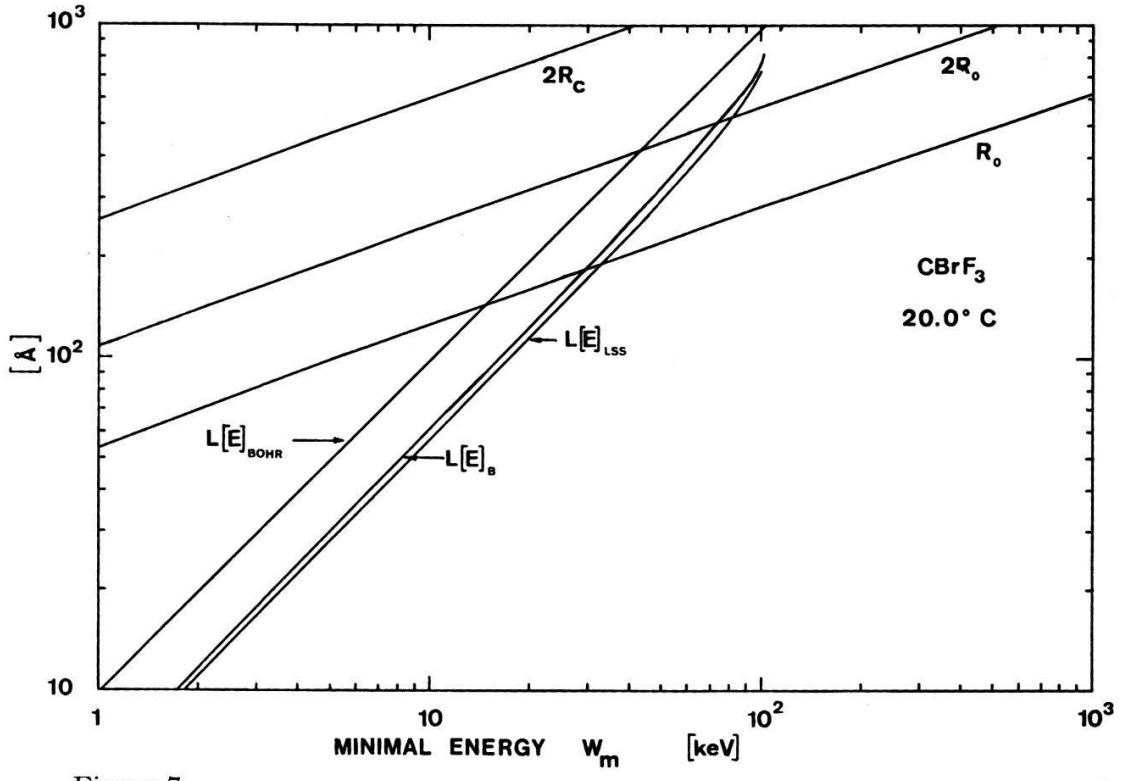

Figure 7

The path length $L(E)$ of the recoiling Pb^{206} as a function of the energy W_m. $L(E)_B$, $L(E)_{LSS}$ and $L(E)_{\text{Bohr}}$ are the path lengths obtained according to the theories of Biersack, Lindhard et al. and Bohr. The critical bubble diameter, the subcritical bubble radius are also drawn in the figure.

The experimental results of the bubble formation induced by recoiling Pb^{206} atom are shown in Figures 8, 9 and 10 for $CBrF_3$, CCl_2F_2 and C_3F_8, respectively.

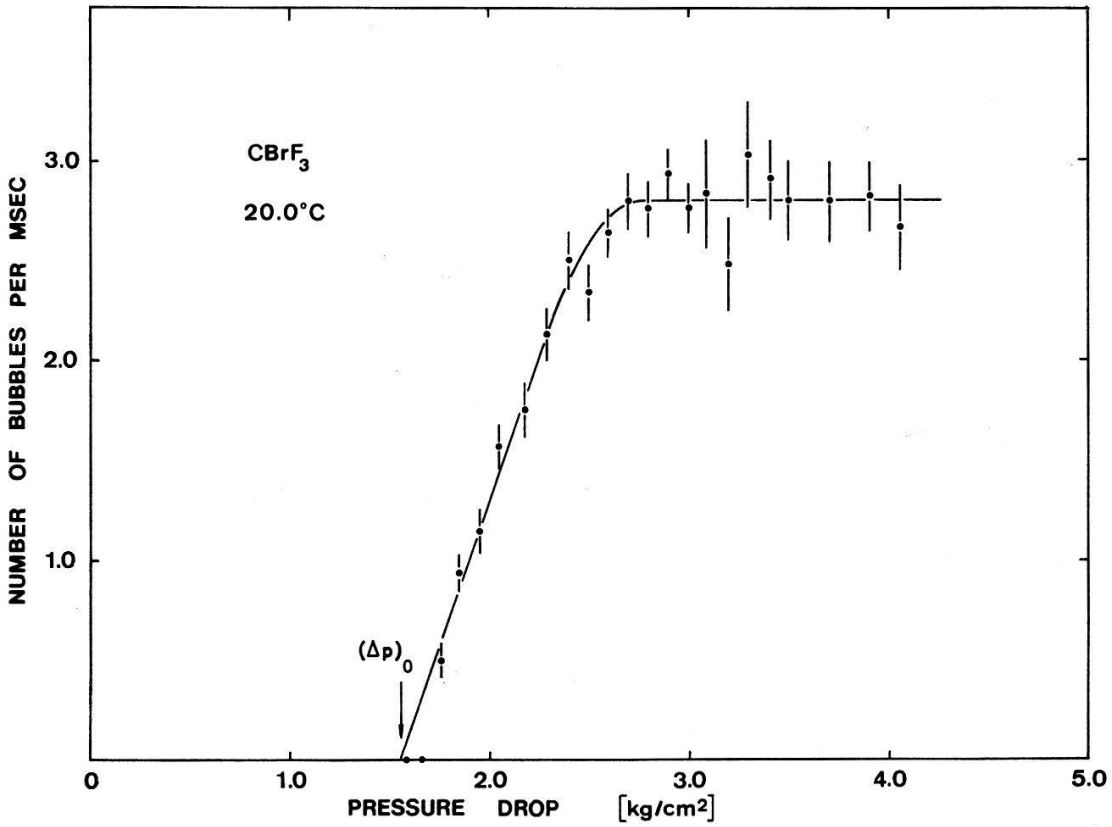

Figure 8
The number of bubbles as a function of the pressure drop for $CBrF_3$ at 20.0 °C.

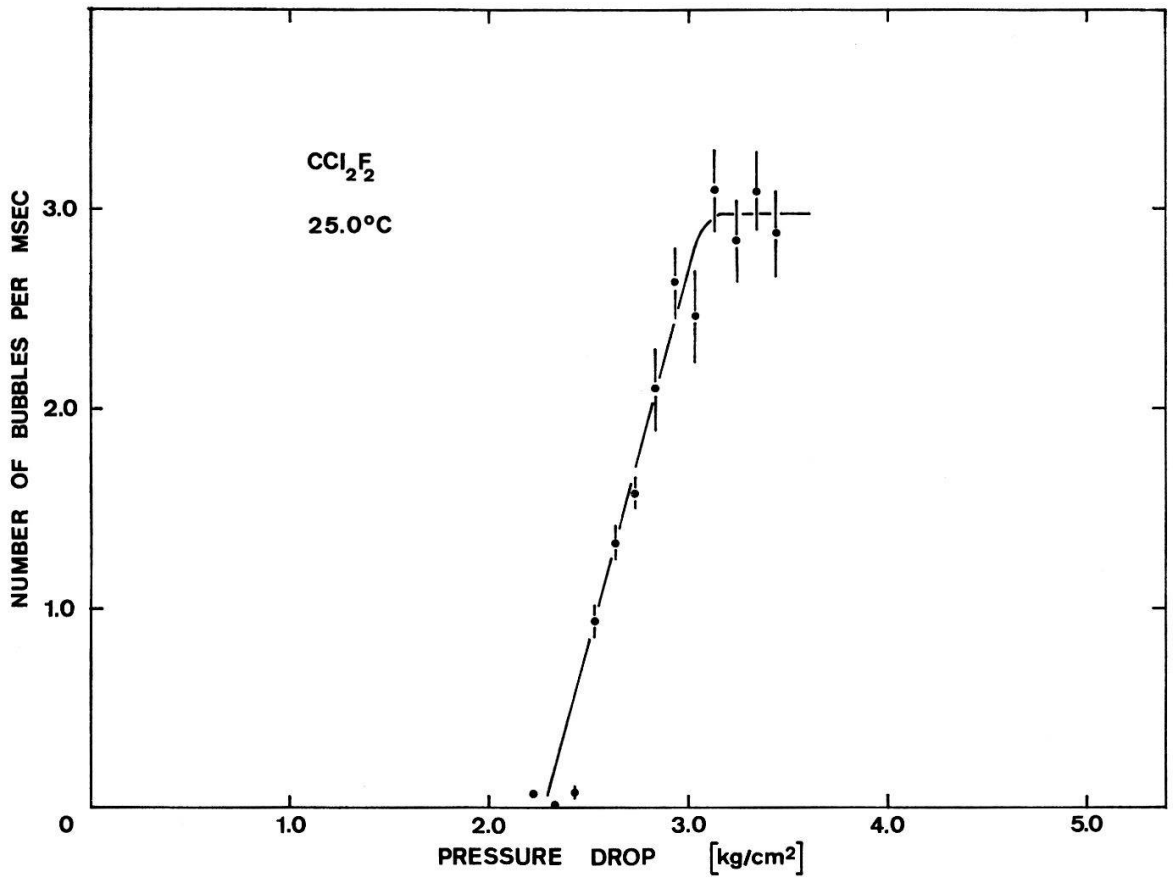

Figure 9
The number of bubbles as a function of the pressure drop for CCl_2F_2 at 25.0 °C.

In analogy to the preceeding chapter an efficiency $\overline{w}(E)$ can be defined as

$$\overline{w}(E) = \frac{N_b(T, \Delta p)}{N_m} \tag{14}$$

where $N_b(T, \Delta p)$ is the number of bubbles and N_m is the number of bubbles at the plateau. The activity of the α-active substance in the liquid has been estimated based on the specific activity of the active substance and loss due to filters and the result of our estimate gives an indication that N_m is equal to the α-activity in the liquid.

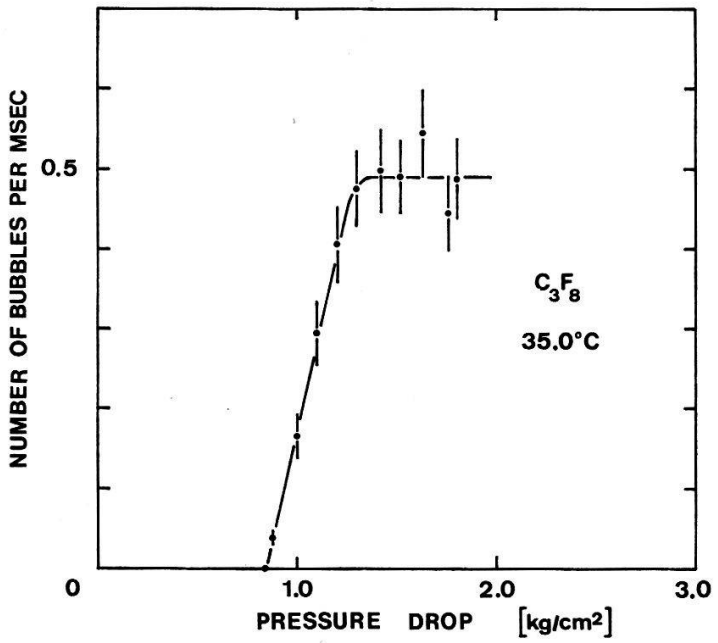

Figure 10
The number of bubbles as a function of the pressure drop for C_3F_8 at 35.0 °C.

Comparing the efficiency $\overline{w}(E)$ of the recoiling atom for the bubble formation to $T(E)$, where $T(E)$ is the ratio of the path length $L(E)$ to the subcritical radius R_0, one finds that the efficiency approaches one for a value of $T(E) = 1$. Figure 11 shows the efficiency $\overline{w}(E)$ as a function of the minimal energy W_m. $T(E)$ are also drawn in the figure, which are calculated according to the theories of Bohr, Lindhard et al. and Biersack. Due to the uncertainty in the range-energy relation it is difficult to conclude on which condition the energy deposition should be made, i.e. within the subcritical volume or within a volume larger than the subcritical volume, but still less than the critical volume. From the results of this investigation it seems that in order to get a 100% efficiency the energy required for the bubble formation should be deposited within a linear interval of approximately R_0. The same behaviour is also true for the other liquids, i.e. CCl_2F_2 and C_3F_8.

The onset of the bubble formation is defined as the value of the pressure drop $(\Delta p)_0$ when the efficiency $\overline{w}(E) = 0$, i.e. extrapolating the slope of the pressure drop curve down to zero number of bubbles, e.g. as shown in Figure 8. It means that for a degree of superheat (pressure drop) $\Delta p < (\Delta p)_0$ bubbles are energetically impossible to be formed and on the other hand for a degree of superheat $\Delta p \geqslant (\Delta p)_0$ bubbles are energetically possible to be formed with the corresponding efficiency $\overline{w}(E)$. This onset of the bubble formation corresponds to the value of the degree of superheat, which, the energy supplied by the recoiling atom, would provide according to the equation (2).

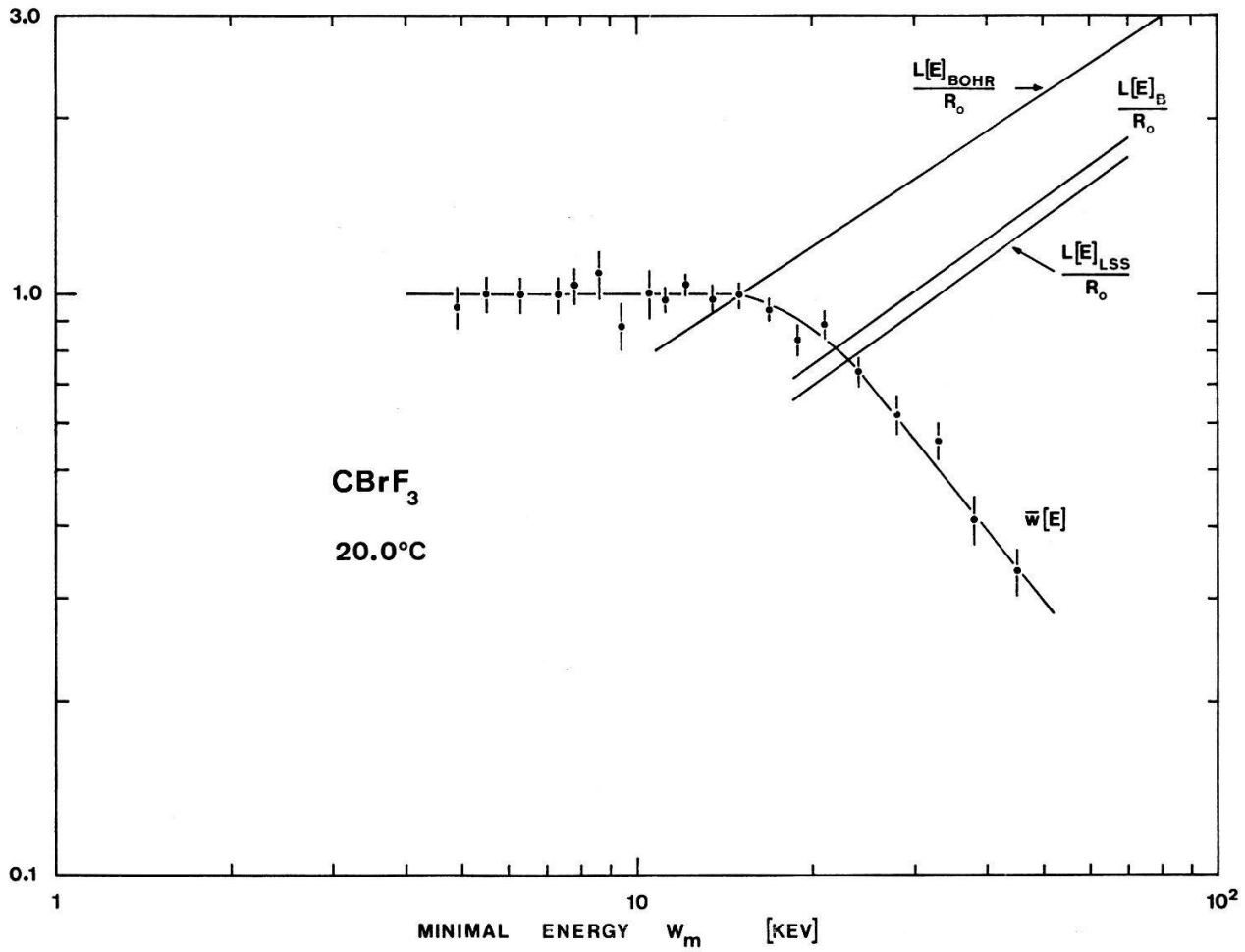

Figure 11
The efficiency $\bar{w}(E)$ of Pb^{206}-recoils for the bubble formation in $CBrF_3$ at 20.0 °C as a function of the minimal energy W_m. The ratio of the path length $L(E)$ to the subcritical radius is also shown in the figure.

The dependence of the onset of the bubble formation $(\Delta p)_0$ on the temperature of the liquid is shown in Figure 12. The full drawn lines in the figure are the theoretical predictions as calculated according to the relation (2). The experimental points as drawn in Figure 12 were not corrected for the temperature change of the liquid during the expansion. If we use the experimental value as given by Johansson [7] for the correction of our experimental results, it is expected that our experimental results would lie on the full drawn line as indicated on the Figure 12. The dashed curves drawn in the figure indicate the values of the pressure drop where the α-decay-recoils reach a 100% efficiency for the nucleation and the shaded area indicates the region where the bubbles are created with efficiency between 0–100%.

4.3 *Bubble formation induced by light*

When a high intensity light beam passes the chamber liquid, bubbles are created within the light beam. Figure 13 shows such an effect in $CBrF_3$, when a pulsed laser light beam traverses the liquid. The energy carried by the laser beam was 60 mJ and the liquid was at 42.0 °C, which was expanded to a stabilization pressure of 15.6 atm corresponding to a pressure drop of 7.8 atm. Using a spark type light source, the same effect was observed, i.e. bubbles are created within the light beam. Since the laser

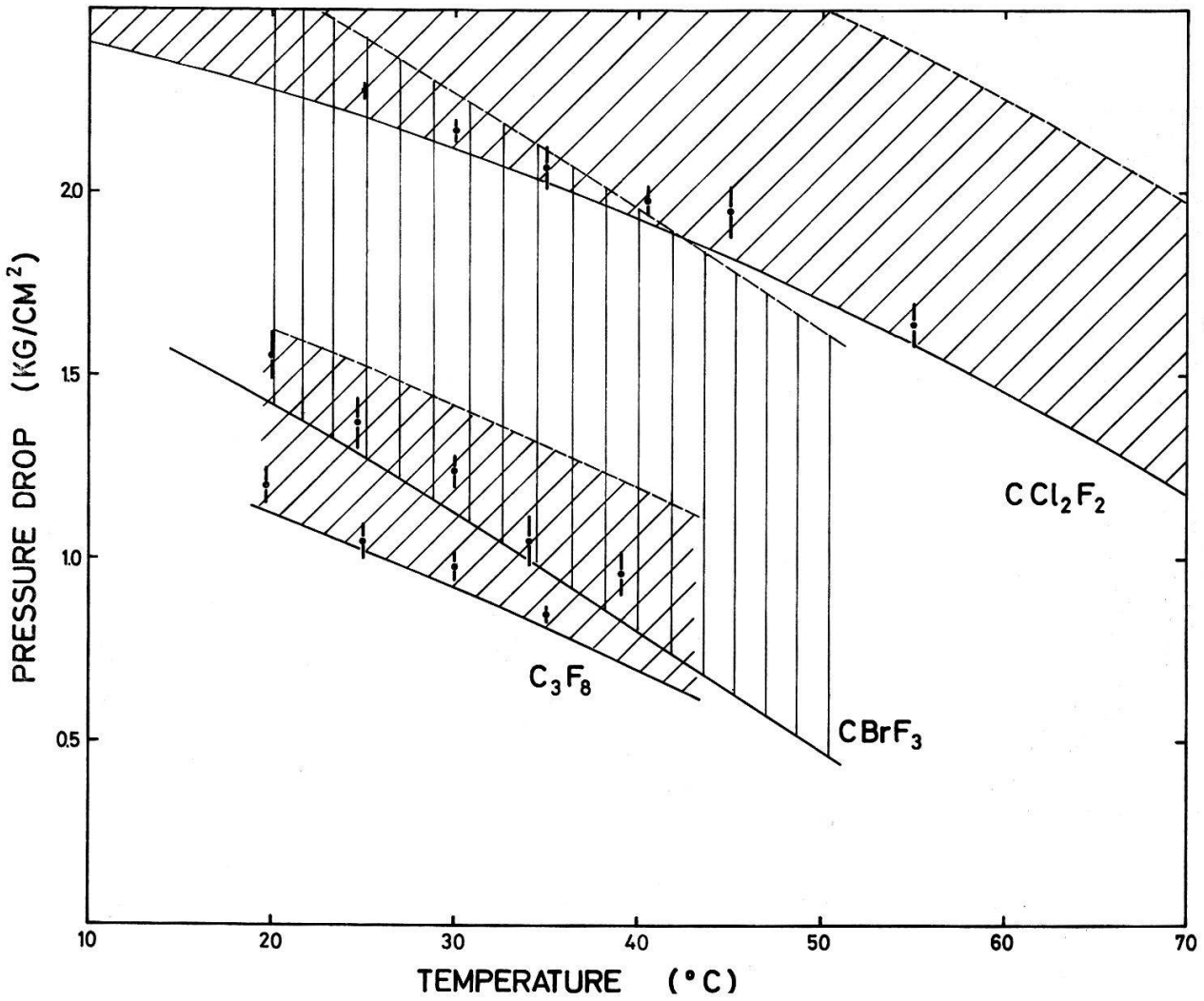

Figure 12
The dependence of the onset of the bubble formation $(\Delta p)_0$ on the temperature of the liquid for $CBrF_3$, CCl_2F_2 and C_3F_8. The full drawn lines are the theoretical predictions according to the equation (2). The dashed curves indicate the values of the pressure drop with a 100% efficiency and the shaded area indicates the region where the bubbles are created with efficiency between (0–100%).

used in our experiment shows two distinct properties, which complicate the interpretation of the experimental results, the laser was then abandoned in favour of a spark type light source. In fact, the laser used in our experiment exhibits a train of sharp spikes of irregular spacing and amplitude, which are not reproducible, and the light distribution is not at all uniform over the entire surface of the laser rod.

The total number of bubbles created in the liquid by the pulsed spark light as a function of the pressure drop is shown in Figure 14. It can be seen in this figure that the total number of bubbles decreases continuously with decreasing pressure drop.

Varying the intensity of the light beam by inserting a neutral density filter into the beam the number of bubbles decreases approximately exponentially with decreasing intensity (see Fig. 15). It seems that the bubbles induced by light are formed nonlinearly with respect to the intensity of the light beam.

Using a pigmented glass long wave pass filter (Jena Schott filters), which cuts sharply the visible spectrum at a certain wavelength, one obtains a remarkable

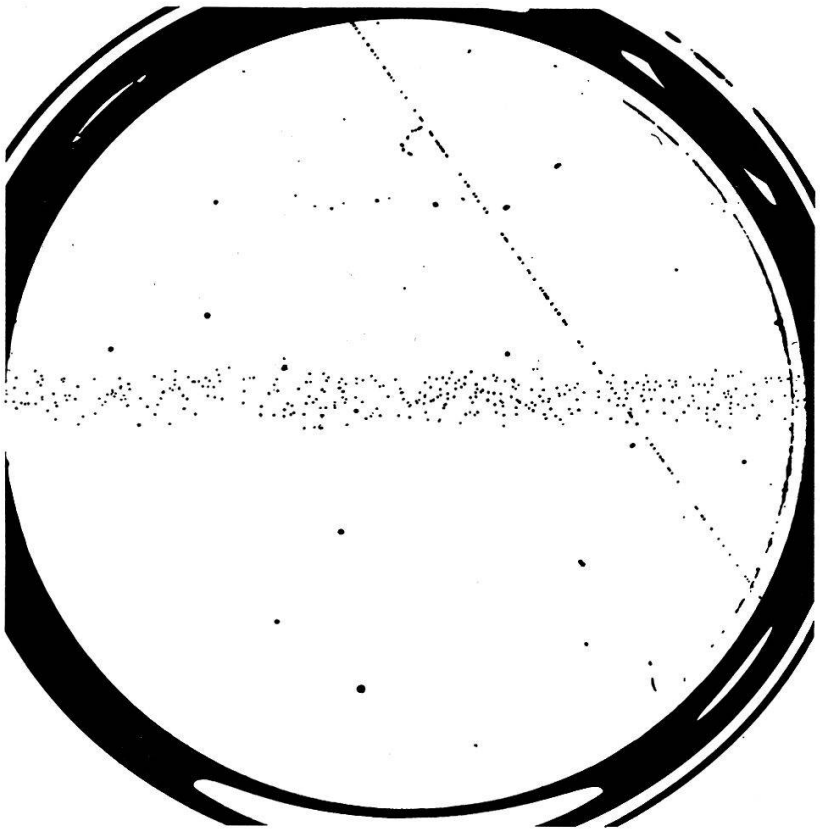

Figure 13
A coincidence event of cosmic ray bubbles and ruby laser bubbles in $CBrF_3$ at 42.0 °C. The degree of superheat of the liquid was 7.8 atm and the laser pulse energy was 60 mJ.

similarity between the differential number of bubbles with the spectrum of the air spark discharge [16] (see Fig. 16). This result seems to indicate that the bubble formation induced by light is independent of the wavelength of the light.

The minimal energy required for the bubble formation far exceeds the energy supplied by a single light quantum, e.g. the minimal energy required for forming a

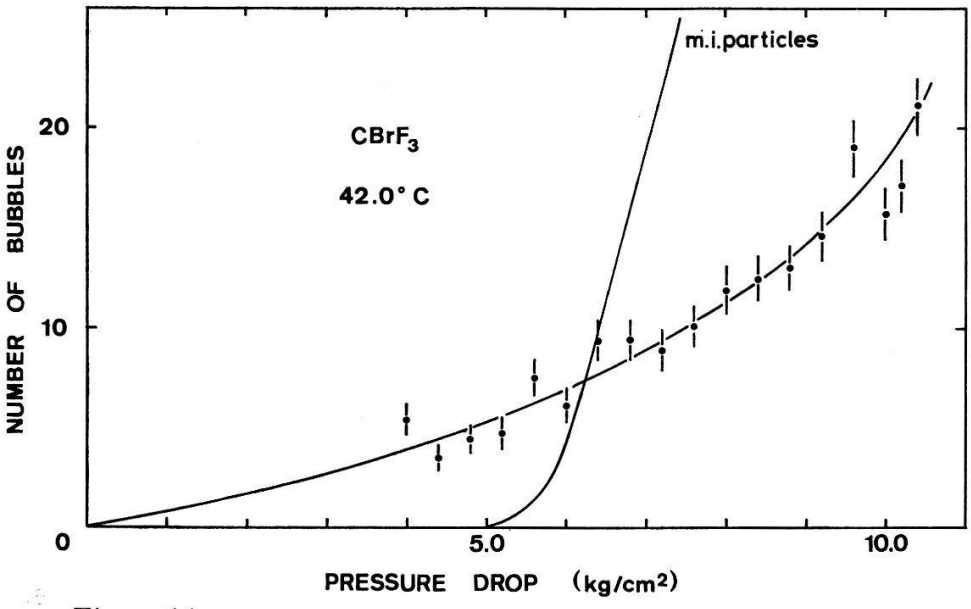

Figure 14
The dependence of the number of bubbles on the pressure drop in $CBrF_3$ at 42.0 °C. The light source was a spark type having an energy of ~0.2 joules. The bubble density for minimum ionizing particles is also shown in the figure.

bubble of radius 60 Å is ~ 200 eV for $CBrF_3$ at 42 °C, whereas the energy of the light quanta is in the energy interval (1.6–3.2) eV.

The energy carried by the light beam which goes into the bubble chamber, is approximately 0.5 joules. The flash duration of the spark light source is approximately 30 μs. Therefore, the intensity of the light beam is approximately equal to 1.4×10^{23} eV/cm²s.

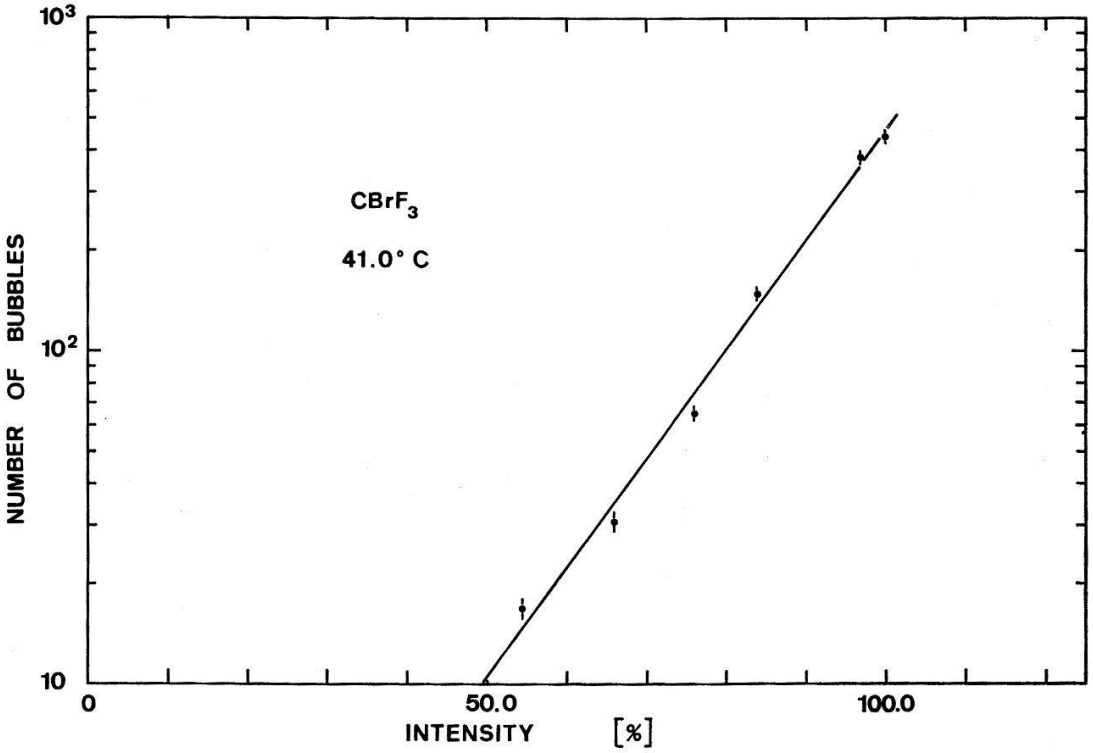

Figure 15
The dependence of the number of bubbles on the intensity of the light beam in $CBrF_3$ at 41.0 °C.

In traversing a liquid layer x the intensity of the light beam in case of a parallel light beam is attenuated according to the following relation

$$I = I_0 e^{-\mu x} \tag{15}$$

where I_0 and μ denote the initial intensity value and the absorption coefficient of the liquid respectively.

The absorption coefficient of the liquid $CBrF_3$ for the visible light as it was determined in this laboratory, is equal to $\sim 2 \times 10^{-2}$ cm^{-1}. The relaxation time of the heat pulse of $CBrF_3$ at 42.0 °C is 2.5 ns for a bubble radius of 60 Å. Therefore, the mean absorbed energy within the relaxation time in a bubble of radius of 60 Å is equal to $\sim 3 \times 10^{-5}$ eV. This is clearly insufficient for the bubble formation.

It is seen above that averaging the energy over a unit volume of a homogeneous liquid does not explain the phenomena. But it is possible that the energy distribution in the liquid undergoes a fluctuation.

An estimate on the fluctuation of the energy distribution in the liquid assuming the Poisson's distribution shows that it is even impossible to describe that the bubbles

are formed due to fluctuation of the energy distribution. From the above consideration, it is unlikely that the bubbles are created in a homogeneous liquid.

Askaryan et al. [37] have observed the formation of bubbles in water, when a laser beam traverses the liquid. They explain that these bubbles are caused by the inhomogeneities in the liquid, which are opaque to the visible light. The same conclusion has also been put forward by Stamberg et al. [13] for the case of bubble formation in the bubble chamber. Such inhomogeneities can be strongly heated and serve as centres for the local heating, vaporization and boiling of the liquid.

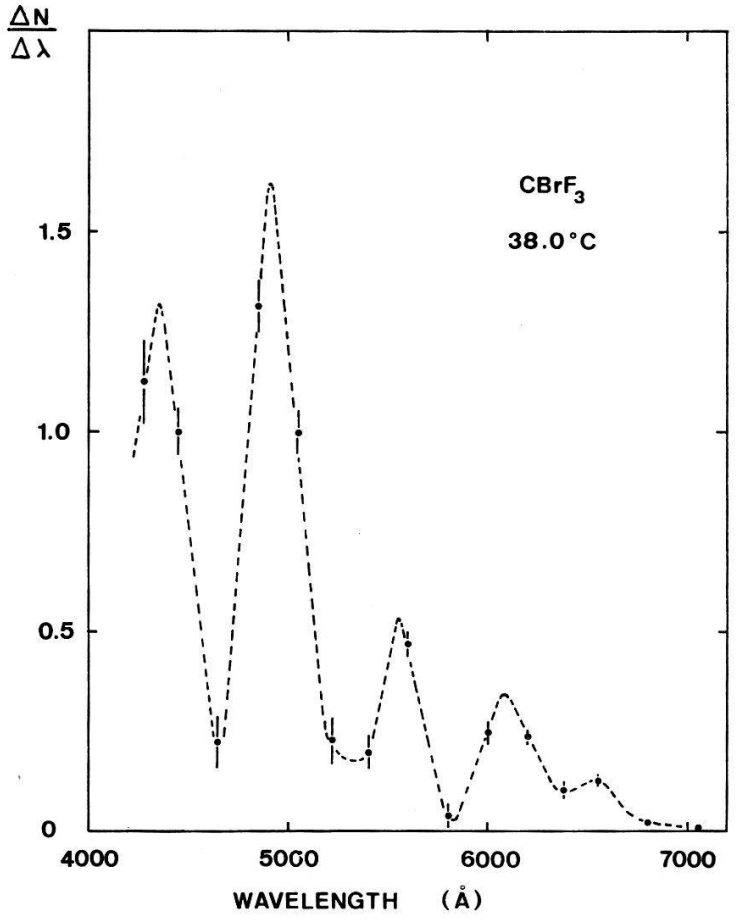

Figure 16
The differential number of bubbles as a function of the wavelength in $CBrF_3$ at 38.0 °C.

The order of magnitude of the beam intensity required for the formation of bubbles on inhomogeneities can be estimated. If the diameter of the inhomogeneity $a \geqslant \delta$, the intensity $I = \varepsilon(\varkappa/\delta)$ and if $a \ll \delta$, $I = \varepsilon(\varkappa/\delta)\,(\delta/a)^2$. δ is the thickness of the liquid layer, which should be vaporized in order to create a bubble of specific size, and $\varkappa$ and ε denote the thermal conductivity of the liquid and the evaporation heat for a unit volume, respectively.

If one takes $a \sim \delta \sim 10^{-3}$ cm for $CBrF_3$ at 38.0 °C, where the thermal conductivity $\varkappa = 0.4 \times 10^{-3}$ cm²/s and $\varepsilon = 1.3 \times 10^{8}$ erg/cm³ the intensity required is given by

$$I = 3.27 \times 10^{19}\ \text{eV/cm}^2\text{s}\,.$$

On the other hand the intensity of the spark light beam available is 1.4×10^{23} eV/cm²s, and this is large enough to create bubbles around an inhomogeneity.

5. Concluding Remarks

As shown in Figure 6, as far the extrapolation of the average efficiency $\overline{w}(E)$ down to low energy region is justified, it can be assumed that the efficiency of the δ-electrons to form a critical bubble approaches one if the energy supplied by the δ-electrons should be deposited within a volume of R_0 diameter. In the case of an α-decay-recoils experiment the same condition seems to be prevalent. Due to the lack of precise knowledge on the energy deposition in the liquid of δ-electrons and of α-decay-recoils, the above results give only a qualitative picture of the condition of the initial stage of bubble formation.

Acknowledgements

For the realization of this study, Prof. Dr. O. Huber is gratefully acknowledged in having taken constant interest in it.

It is also a great pleasure to thank Prof. Dr. B. Hahn for his encouragements and for the many opportunities to have useful discussions, which certainly have contributed to the work presented here.

It should be also mentioned here the contributions offered by very many people, who have given much of their precious time to discuss the various problems and valuable assistance particularly rendered by Messrs. H. Jungo and P. Heimo in having constructed the bubble chamber and many other experimental apparatus.

Also the contributions and assistance of Mrs. T. Chassot and the scanning staff at the University of Berne are herewith very highly appreciated.

The numerical calculations were executed at the computer of the Automation Institute of the University of Fribourg and at CERN. Their collaboration and help during the course of this study are greatly acknowledged.

It is a pleasure to thank Miss M. B. Sauter for rendering the patchwork manuscript into legible form.

This work was supported by the Swiss National Science Foundation.

REFERENCES

[1] F. Seitz, Phys. Fluids *1*, 2 (1958).
[2] G. Riepe and B. Hahn, Helv. phys. Acta *34*, 865–892 (1961).
[3] P. Kunkel, Doctoral Thesis Würzburg, 1967.
[4] E. Hugentobler, B. Hahn and F. Steinrisser, Helv. phys. Acta *36*, 601–621 (1963).
[5] D. A. Glaser, *Handbuch der Physik*, Vol. XLV (1958).
[6] D. V. Bugg, Prog. in Nucl. Phys., Vol. 7, ed. O. Frisch (Pergamon Press, London 1959), p. 1.
[7] B. Alfredson and T. Johansson, Arkiv Fysik *19*, 383 (1961); T. Johansson, Arkiv Fysik *19*, 397 (1961).
[8] A. G. Tenner, Nucl. Instrum. Meth. *22*, 1–42 (1963).
[9] T. Johansson, Arkiv Fysik *28*, 461 (1965).
[10] J. Hofmann and E. Hugentobler, Helv. phys. Acta *38*, 783 (1965).
[11] Ch. Peyrou, *Bubble and Spark Chambers*, ed. R. P. Schutt (Academic Press, New York 1967), p. 19.
[12] E. Hugentobler, R. F. H. Poesposoetjipto, B. Hahn, H. P. Brändli, R. Dändliker and K. P. Meyer, Helv. phys. Acta *37*, 226 (1964).
[13] R. C. Stamberg and D. E. Gillespie, J. appl. Phys. *37*, 459 (1966).

[14] B. Hahn, A. W. Knudsen and E. Hugentobler, Nuovo Cim. *15*, Suppl. 2 (1960).
[15] M. Guillot, J. Chim. Phys. *28*, 92 (1931).
[16] M. P. Vanyukov, V. R. Muratov and I. A. Mukhitdinova, Optics and Spectroscopy *10*, 294 (1961).
[17] G. Glaser, Optik *1*, 33 (1950).
[18] J. Frenkel, *Kinetic Theory of Liquids* (Dover Publication 1955).
[19] 'Freon' Technical Bulletin B-29, T-13B1, T-12, E.I. Du Pont de Nemours, Delaware.
[20] General Chemical, Technical Bulletin TB-85602 (1955).
[21] General Chemical, Technical Bulletin PD-TA-218-4-59.
[22] S. Ono and S. Kondo, *Handbuch der Physik*, Vol. X (1960).
[23] D. E. Lea, *Actions of Radiations on Living Cells* (Cambridge University Press, 1956), p. 24.
[24] H. A. Bethe, *Handbuch der Physik*, Vol. XXIV/1 (1933), p. 273–560.
[25] Chr. Møller, Ann. Phys. *14*, 531 (1932).
[26] N. Bohr, Matt. Fys. Medd. Dan. Vid. Selsk. *18*, 8 (1948).
[27] J. Lindhard, M. Scharff and H. E. Schiøtt, Matt. Fys. Medd. Dan. Vid. Selsk. *33*, 14 (1963).
[28] J. P. Biersack, Hahn-Meitner-Institut für Kernforschung, Berlin, HMI-B-37 (1964).
[29] J. P. Biersack, Z. Phys. *211*, 495–501 (1968).
[30] L. Winsberg and J. M. Alexander, Phys. Rev. *121*, 518–528 (1961).
[31] J. M. Alexander and L. Winsberg, Phys. Rev. *121*, 529–537 (1961).
[32] D. Powers and W. Whaling, Phys. Rev. *126*, 61 (1962).
[33] D. Marx, Z. Phys. *195*, 26–43 (1966).
[34] D. Powers, W. K. Chu and P. D. Bourland, Phys. Rev. *165*, 376 (1968).
[35] W. K. Chu, P. D. Bourland, K. H. Wang and D. Powers, Phys. Rev. *175*, 342 (1968).
[34] D. Powers, W. K. Chu and P. D. Bourland, Phys. Rev. *165*, 376 (1968).
[35] W. K. Chu, P. D. Bourland, K. H. Wang and D. Powers, Phys. Rev. *175*, 342 (1968).
[36] H. E. Schiøtt, Matt. Fys. Medd. Dan. Vid. Selsk. *35*, 9 (1966).
[37] G. A. Askaryan, A. M. Prokhorov, G. F. Chanturiya and G. P. Shipulo, Soviet Phys. JETP *17*, 1463 (1963).